Linear and nonlinear electronic transport in weakly insulating double layered manganites

K. B. Chashka, B. Fisher, J. Genossar, A. Keren, L. Patlagan, and G. M. Reisner
Physics Department and Crown Center for Superconductivity, Technion, Haifa 32000, Israel

E. Shimshoni
Department of Math-Physics, Oranim-Haifa University, Tivon 36006, Israel

J. F. Mitchell
Materials Science Division, Argonne National Laboratory, Argonne, Illinois 60439
(Received 30 May 2001; revised manuscript received 29 October 2001; published 27 March 2002)

Polycrystalline $La_{1.2}Sr_{1.8}Mn_{2-y}Cr_yO_7$ ($0 \leqslant y \leqslant 0.25$) is a weakly insulating ferromagnet with low-T thermopower of metalliclike values. This combination of properties indicates electronic transport through percolating paths embedded in an insulating medium. The temperature dependence of the resistivity at low T and the nonlinear conductivity obtained from pulsed I-V measurements over a wide range of currents are consistent with inelastic tunneling through intergrain or intragrain weak links that disrupt the percolating paths. Thermopower and resistivity measurements on two weakly insulating single crystals of $La_{1.4}Sr_{1.6}Mn_{1.85}Cr_{0.15}O_{7-\delta}$ and the I-V measurements on the more resistive crystal exhibit features very similar to those found in the polycrystals. In single crystals the nonlinearity of conductivity is pronounced under much lower electric fields than in polycrystals.

DOI: 10.1103/PhysRevB.65.134441 PACS number(s): 72.20.Ht, 72.20.Pa, 73.40.Gk, 75.30.Vn

I. INTRODUCTION

The metal-insulator mixed-phase character of the manganites and the percolative electronic transport associated with it, are supported by experiments[1] and models and lead to a rather simple and intuitive explanation of their remarkable magnetotransport properties.[2] The temperature dependence of the resistivity $[\rho(T)]$ of an optimally doped manganite exhibits a crossover from a negative temperature coefficient above the Curie temperature (T_c), to a positive temperature coefficient below T_c. Departure from optimal doping or various partial substitutions for Mn by $3d$ ions affect mostly the resistivity in the low-T regime. Away from optimal doping the maximum of $\rho(T)$ observed close to T_c degenerates gradually into a bend at the crossover from a high to a low negative temperature coefficient. The most remarkable feature of the low-T regime is the combination of high resistivity, weakly dependent on temperature, with small, metalliclike values of the absolute thermopower (S). Since the thermopower is a very sensitive probe of the conducting component of the mixed-phase material, and is little affected by geometry and grain boundaries,[3] this behavior indicates that electronic transport is carried through a percolating network of high conductivity channels embedded in an insulating medium. However, unlike the thermopower, the resistivity is dominated by weak links distributed along the conducting paths.

This ''weakly insulating'' regime is interesting, since its main features have been observed in the past in a number of systems, some of them unrelated to the manganites.[4] The advantage of studying this regime in manganites is the abundance of relevant information. Recently we studied polycrystalline $La_{0.7}Sr_{0.3}Mn_{1-y}Fe_yO_3$ ($y=0.16$–0.18);[5] its parent material $La_{0.7}Sr_{0.3}MnO_3$ is a pseudocubic, optimally doped manganite.[6] The temperature dependence of magnetization, resistivity and thermopower of $La_{0.7}Sr_{0.3}Mn_{1-y}Fe_yO_3$ ($y=0.16$–0.18) exhibit the features of mixed-phase state and of percolating electronic transport discussed above. Pulsed I-V measurements carried out on this system in the low-T regime showed that the current density (J) increases faster than linearly with electric field $\mathcal{E}$; the excess current density $\Delta J = J - \sigma\mathcal{E}$ (where σ is the Ohmic conductivity) obeys a power-law dependence on $\mathcal{E}$. At 20 K $\Delta J \propto \mathcal{E}^{2.3\pm0.1}$ was obtained for all samples. For $y=0.18$ we obtained $\rho \propto T^{-p}$ ($p \approx 4/3$). This behavior is consistent with the theory of Glazman and Matveev[7] (GM) for tunneling across thin amorphous films; for inelastic tunneling via two localized states it predicts that $\Delta I \propto V^{7/3}$ and that the excess conductance $\propto T^{4/3}$. The GM model was shown to fit remarkably well the results of transport measurements carried out on *individual grain boundaries* in a manganite.[8] Surprisingly, our results for polycrystalline $La_{0.7}Sr_{0.3}Mn_{1-y}Fe_yO_3$ indicated that this model may be extended also to a network of weak links. We tentatively identified the weak links with grain boundaries.[5]

The polycrystals and single crystals of $La_{2-2x}Sr_{1+2x}Mn_{2-y}Cr_yO_7$, investigated in the work reported here belong to naturally layered manganites, $(R,A)_{n+1}Mn_nO_{3n+1}$ (R rare earth; A alkaline earth ions) which are presently intensively studied due to their two-dimensional nature. Since the publication of Ref. 9, interest has been focused on double-layered manganites ($n=2$) and, in particular, on $La_{1.2}Sr_{1.8}Mn_2O_7$.[10] Below T_c, the ratio of the resistivities measured perpendicular to the planes and in the planes of a single crystal is about 100. Thus, polycrystalline material of this type is expected to be weakly insulating due to the large resistivity anisotropy; with the conductivity tensor's axes of the crystallites pointing in random directions in space, even the optimally doped material appears as if it were phase separated. And indeed, in the FM state, the resistivity of polycrystaline $La_{1.2}Sr_{1.8}Mn_2O_7$ is high;[11] partial

substitution of Mn by Cr induces in the FM state a monotonic increase of ρ as a function of y.[11] Therefore, the $La_{1.2}Sr_{1.8}Mn_{1-y}Cr_yO_7$ system seemed to us very suitable for the study of percolative, linear, and nonlinear electronic transport in a phase-separated medium. One of the main objectives of this work was to compare the transport properties and nonlinear conductivity of the polycrystals with those (in the *a-b* plane) of weakly insulating single crystals of similar composition.

We carried out a systematic study of the temperature dependence of the magnetization, resistivity, and thermopower of polycrystalline $La_{1.2}Sr_{1.8}Mn_{1-y}Cr_yO_7$ $(0 \leqslant y \leqslant 0.25)$. These measurements showed that while magnetization decreases and resistivity increases (by orders of magnitude) with Cr doping, the low-T thermopower remains almost identical for all samples.

We investigated the thermopower and the resistivity in the *a-b* plane of two weakly insulating single crystals of $La_{1.4}Sr_{1.6}Mn_{1.85}Cr_{0.15}O_{7-\delta}$. They exhibit features very similar to those of the polycrystals; although the low-T resistivities of the two crystals differ by up to two orders of magnitude, their thermopowers are very low and almost identical. This indicates that electronic transport is percolative in both the polycrystals and in single crystals. For all the investigated samples (polycrystals as well as single crystals), the experimental results indicate that electronic transport at low-T is governed by similar mechanisms. The detailed analysis of the results is consistent with transport dominated by tunneling through weak links (WL), which may be of intergrain and/or intragrain origin.

The sample preparation and experimental techniques employed in this work are presented in Sec. II. Our efforts to eliminate spurious Joule heating effects in the *I-V* characteristics are emphasized. The results are discussed in detail in Sec. III A for polycrystals and in Sec. III B for the single crystals. The experimental results and the conclusions drawn from their analysis are summarized in Sec. IV.

II. EXPERIMENT

High quality ceramic samples of $La_{1.2}Sr_{1.8}Mn_{2-y}Cr_yO_7$ ($y=0$, 0.1, 0.15, 0.2, and 0.25) were prepared essentially according to the original protocol;[11] the grinding-annealing cycles were repeated until the x-ray powder-diffraction spectra showed no traces of impurities or foreign phases. The lattice parameters fit well earlier reports.[11] Single crystal (SC) platelets were separated from a boule grown from a $La_{1.2}Sr_{1.8}Mn_{1.75}Cr_{0.25}O_7$ rod by the floating zone method, as described in Ref. 12. The platelets selected for measurements (SC1 and SC2) belong to the same region of the rod. Energy dispersive spectroscopy spectra obtained from several spots of each of the platelets confirmed their chemical homogeneity and determined their composition as $La_{1.4}Sr_{1.6}Mn_{1.85}Cr_{0.15}O_{7-\delta}$, slightly different from that of the starting material. Magnetization, resistivity, thermopower, and pulsed *I-V* measurements were carried out as described in Ref. 5.

For $\rho(T)$ and *I-V* measurements we used bar-shaped polycrystalline samples and rectangular single crystalline platelets with four-probes attached to them. Special care was taken of the quality of the current contacts and the voltage probes in order to prevent Joule heating at the current contacts and to eliminate electric-field inhomogeneity at both types of contacts. At low currents dc measurements were carried out using an XYY recorder. At high currents, the measurements were carried out using single current pulses of durations in the millisecond range, from a Keithley 237 high voltage source. The time dependence of the voltage drops between ground and each of the voltage probes, were recorded using simultaneously the two channels of a Tektronix 2221A digital storage oscilloscope. The current was checked during a second pulse by the voltage drop across a small resistance in series with the sample. Beyond the finite rise time (in the microsecond range), the measured voltages showed no time dependence during the current pulses. The lower current range of the pulsed measurements overlapped the dc measurements. The differences between the dc and the pulsed measurements become significant already for current densities as low as a few A/cm^2; negative differential resistance was obtained from dc measurements with currents in the range where, in pulsed measurements, the nonlinearity of the *I-V* traces was barely observed. In percolative current flow the *local* current density is much higher than the *average* current density; accordingly, the local temperature may be far above the average temperature of the sample. The only reliable test for the absence of Joule heating is the time independence of the voltage drop during the current pulses.[13]

III. EXPERIMENTAL RESULTS AND DISCUSSIONS

A. Polycrystalline samples of $La_{1.2}Sr_{1.8}Mn_{2-y}Cr_yO_7$ ($y=0$, 0.1, 0.15, 0.2, and 0.25)

1. Temperature dependence of magnetization, resistivity, and thermopower

The magnetization M, measured at 0.05 T, the Ohmic resistivities ρ, and the absolute thermopower S, of samples of compounds prepared in this work are plotted as functions of temperature in Figs. 1(a)–1(c), respectively. The points marked by bold squares in Fig. 1(a) represent T_c [defined as $T(\partial^2 M/\partial T^2 = 0)$]. In agreement with Ref. 11, T_c is the lowest for $y=0$; for $0.1 \leqslant y \leqslant 0.25$ it is practically independent of Cr content. For $120 \leqslant T \leqslant 200$ K M $(y=0)$ is almost constant; deviation from the Curie-Weiss law above T_c has been observed in the past and was attributed to the presence of short-range ferromagnetism.[14,16] Apparently, Cr doping suppresses this short-range order but has little effect on the onset of long-range order. With increasing y the maximal magnetization M_{max} at 0.05 T decreases at a moderate rate (extrapolation shows that $M_{max} \to 0$ for $y \approx 1$). In polycrystalline Cr-free $La_{1.2}Sr_{1.8}Mn_2O_7$, the magnetization measured at 5 K and 6 T [see inset in Fig. 1(a)] is about 1/2 of the saturation magnetization measured in the optimal orientation of a single crystal $(H \perp c)$.[14] In view of the strong anisotropy of the crystallites this well represents M averaged over all directions. For $y=0.25$ the saturation magnetization is further reduced by about 40%.

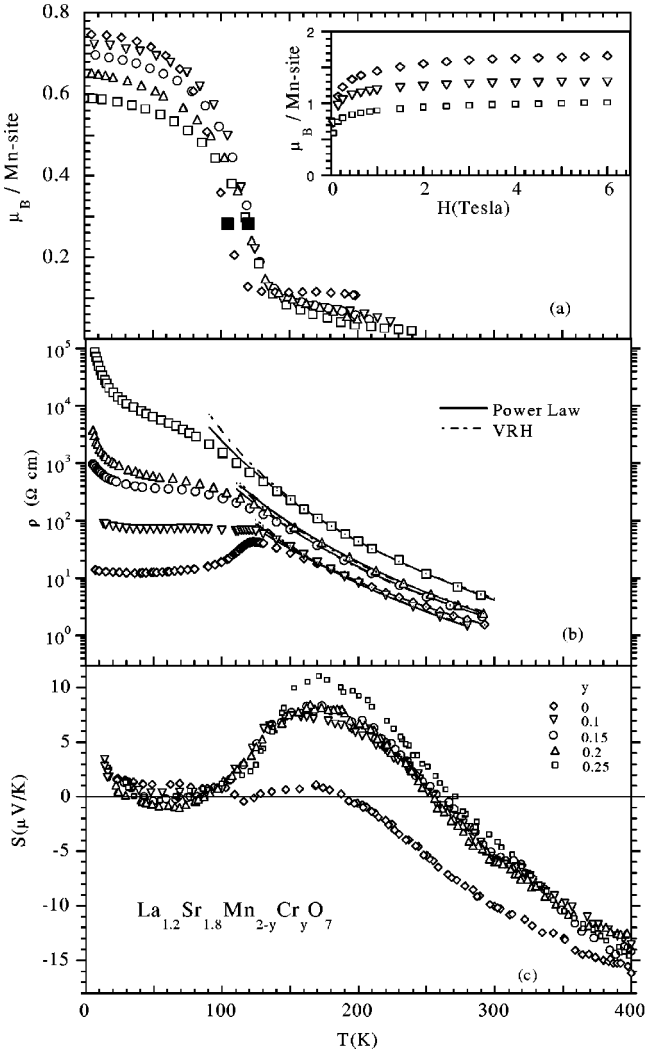

FIG. 1. Temperature dependence of magnetization (a), resistivity (b), and absolute thermopower (c) of polycrystalline samples of $La_{1.2}Sr_{1.8}Mn_{2-y}Cr_yO_7$, for various values of y. The T_c's are marked by bold squares in (a). The inset shows magnetization vs magnetic field for $y=0$, 0.1, and 0.25 at 5 K. The solid and dot-dashed lines in (b) represent fits at high temperatures to a power law or to Mott's law, respectively.

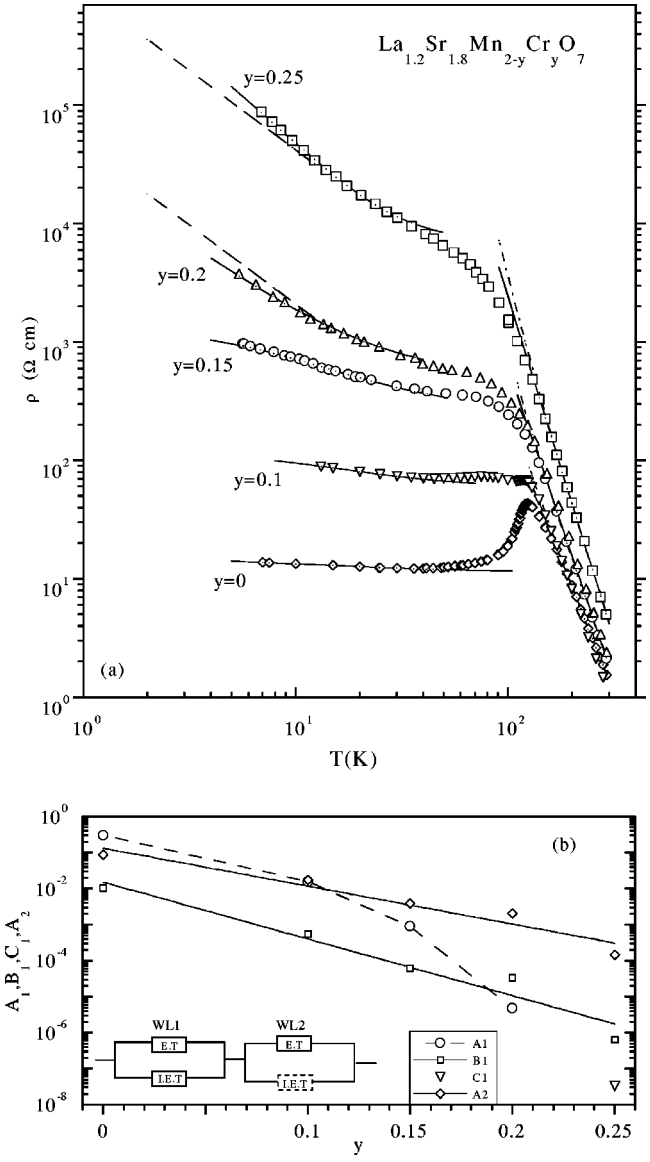

FIG. 2. (a) Temperature dependence of resistivity of polycrystalline samples of $La_{1.2}Sr_{1.8}Mn_{2-y}Cr_yO_7$, on a log-log scale. The dashed lines at low temperatures represent $\rho \propto T^{-4/3}$. As in Fig. 1(b), the solid and dot-dashed lines represent fits at high temperatures to a power law or to Mott's law, respectively. (b) Equivalent circuit of two weak links in series (WL1 and WL2) and parameters [Eq. (2)] of the fitted curves in Fig. 2(a), as a function of composition; ET stands for elastic tunneling and IET for inelastic tunneling. The lines in (b) are guides to the eye.

In Fig. 1(b), $\rho(T)$ plotted on log-linear scale exhibits distinct high- and low-temperature regimes, each with a different temperature dependence. In the narrow range of temperatures between 150 K and room temperature, both a power-law dependence $\rho(T) \propto T^{-p}$ and Mott's law for variable range hopping[15] (VRH), $\rho \propto \exp(T_o/T)^{1/4}$ fit the experimental data almost as well [see solid and dot-dashed lines at the right of Fig. 1(b) and Fig. 2(a)]; a difference is distinguishable only between extrapolations of fitted lines.[17] The crossover from the high-T to the low-T regime is more pronounced in the log-log plot of $\rho(T)$ shown in Fig. 2 that focuses on the low-T regime and will be discussed in detail below.

$S(T)$ for the various compositions is plotted in Fig. 1(c). Above T_c the $S(T)$ data for $y \geqslant 0.1$ are almost identical with S_{ab} (S measured in the ab plane) of a single crystal of $La_{1.2}Sr_{1.8}Mn_2O_7$ (see Fig. 4 in Ref. 16), except for the maximum (S_{max}) around 200 K, which is slightly higher for $y=0.25$. The cusp of $S(T)$ that marks T_c (see Ref. 16) appears on our $S(T)$ plot for $y=0$, but is smeared out for other compositions. At lower temperatures $S(T)$ for all samples ranges between -1 and $+2$ μV/K, while the resistivities increase by about four orders of magnitude with y increasing from 0 to 0.25. The low S (comparable with that of metallic-like single crystal of similar composition[16]) indicates that at low temperatures the Cr substitution has little effect on the electronic structure of the conducting component of the ma-

terial; it seems that its main effect is on the microstructure of the material.

We focus now on the resistivity in the low-temperature regime. With increasing y the log-log plots of $\rho(T)$ in Fig. 2(a) become steeper. At the lowest temperatures the negative slope is slightly less than 4/3 for $y=0.2$, and slightly more for $y=0.25$, (see dashed lines near the corresponding curves). As shown below, this slope is significant and leads to a possible interpretation of the results.

According to the GM model,[7] for $eV \ll k_B T$ the temperature dependence of the conductance G across a thin amorphous film is given by

$$G=(G_o+G_1)+\sum_{n=2}^{\infty} b_n T^{n-2/(n+1)}. \tag{1}$$

The first two terms in Eq. (1) represent elastic tunneling processes: direct tunneling (G_o) and resonant tunneling via one impurity (G_1). The T-dependent terms represent inelastic, multistep tunneling via $n \geqslant 2$ impurities; the power index for $n=2$ is 4/3, for $n=3$ it is 5/2, etc. As temperature increases the contribution of processes with higher n increases. Above a characteristic temperature T_n, the contribution of n-impurity chains to G exceeds that of $n-1$ impurity chains. The ''effective'' power index increases with increasing temperature, eventually leading to a VRH-type behavior.[7] Thus conductance $\propto T^{4/3}$ is a signature of inelastic tunneling across a thin film via two localized states. At low temperatures $\rho(T)$ for $y=0.2$ and $y=0.25$ seem to carry the fingerprints of such regime. Our confidence in the applicability of the GM model for the interpretation of the above measurements rests also on our previous results.[5]

In order to model the system we assume the presence of bundles of percolating ''metallic'' filaments, their resistivity dominated by WL that behave like thin amorphous films. Presumably there is a distribution of WLs along each conducting filament, with various characteristic temperatures T_n. In a first approximation, the complicated network of percolating filaments in our samples is modeled using only two types of WLs (WL1 and WL2), with different characteristic temperatures $T_n(2) \gg T_n(1)$ as in the equivalent circuit shown in Fig. 2(b). This simple model is applicable far below T_c where the ratio conducting/nonconducting material is constant, that is, where the magnetic microstructure is frozen. Thus the measured resistivity is decomposed as follows:

$$\rho(T)=\frac{1}{A_1+B_1T^{4/3}+C_1T^{5/2}+\cdots}+\frac{1}{A_2+B_2T^{4/3}+\cdots}, \tag{2}$$

where the denominators represent the contributions of conductances with elastic and inelastic tunneling acting in parallel. The WLs with $T_2(i)>T$ contribute a constant $1/A_i$ term to the sum of Eq. (2), that is, a temperature-independent term. In Fig. 2(a) the solid lines at low temperature represent fit of Eq. (2) to the experimental curves using the data obtained below 25 K (where the magnetization is almost temperature independent). Each calculated trace is based on only three fitting parameters: A_1, B_1, and A_2 for $y \leqslant 0.2$ and B_1, C_1 and A_2 for $y=0.25$. The fitting parameters are plotted in Fig. 2(b) as functions of y. A_1 drops rapidly with increasing y and apparently a metal-insulator transition [$\sigma(T=0)\rightarrow 0$] occurs at $0.2<y_c<0.25$. The characteristic temperature of WL1 for the crossover from the predominantly resonant tunneling to the regime of inelastic tunneling via pairs of states $T_2(1)=(A_1/B_1)^{3/4}$, decreases with y from ~ 12 K for $y=0$ to 0 K for $y \leqslant 0.25$. This behavior is probably due to the changes in the density of localized states around E_F and in their spatial extent within the barrier.[18]

2. J-$\mathcal{E}$ characteristics

I-V measurements were carried out on polycrystalline bar-shaped samples with typical cross sections of 0.5 mm^2 and lengths of 5–10 mm; the distance between voltage probes was 2-3 mm. Detailed *I-V* characteristics were obtained for temperatures up to 120 K. At higher temperatures, non-Ohmic behavior was observed only close to the upper limit of the available fields.

The J-$\mathcal{E}$ characteristics of a Cr-free sample and a Cr-doped sample with $y=0.25$ are plotted on a log-log scale in Fig. 3(a,b) (for 20 K and 100 K). Full and open circles represent dc and pulsed measurements, respectively. In the range of our measurements, the current through the Cr-free sample is Ohmic over several orders of magnitude of J (the slope is 1); for the doped sample, due to its high resistivity, the Ohmic range is much narrower. The effect of Joule heating is seen best at the top of the dc trace for the undoped sample at 100 K; the portion of the trace above $\mathcal{E} \sim 10$ V/cm maps the temperature dependence of ρ above 100 K: a drop in the slope of $J(\mathcal{E})$ due to positive temperature coefficient at $T<T_c$ is followed by an accelerated increase in J and negative differential resistivity due to negative temperature coefficient of $\rho(T)$ at $T>T_c$, as local temperature of the conduction channels increases.

Nonlinearity of the pulsed J-$\mathcal{E}$ characteristics becomes prominent for $\mathcal{E}>10$ V/cm. As in Ref. 5 we calculated the *excess current density* $\Delta J=J-J_{Ohmic}$ [$J_{Ohmic}=\sigma\mathcal{E}$ is the extrapolated value of the Ohmic current density at high fields—see dashed lines in Figs. 3(a) and 3(b)]. The data of ΔJ (marked by triangles) were plotted as functions of $\mathcal{E}$; it is seen that they fall on steep straight lines, which follow the power law $\Delta J \propto \mathcal{E}^{\alpha}$. Only data from pulsed measurements were used for fitting; these usually cover a range of two to three orders of magnitude in ΔJ [as in Fig. 3(b)]. For the doped sample at 20 K the extrapolation of the fitted line passes through the dc data. In the two insets of Fig. 3 the data for the doped sample at 20 K and for the undoped sample at 100 K are plotted on linear scale that emphasizes the top decades of J and ΔJ.

The four straight lines in Figs. 3(a,b) representing ΔJ vs $\mathcal{E}$ are almost parallel, showing that the values of their power indices α are very close, this, in spite of large differences in composition and temperature and therefore large differences in the Ohmic conductivities. The results may be summarized in terms of two parameters, the power index α and the characteristic field $\mathcal{E}_o$ defined as $\Delta J(\mathcal{E}_o)=\sigma\mathcal{E}_o$. The parameters α and $\mathcal{E}_o$ as functions of temperature for various composi-

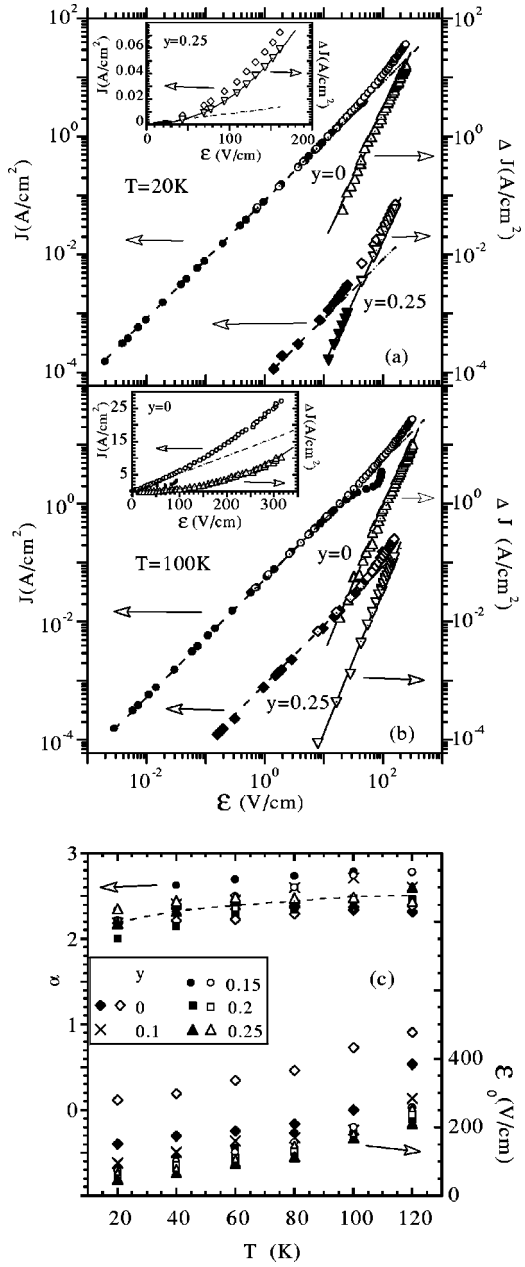

FIG. 3. J-$\mathcal{E}$ characteristics (left y axis) for a Cr-free sample of $La_{1.2}Sr_{1.8}Mn_{2-y}Cr_yO_7$ ($y=0$) and for a sample with $y=0.25$ and the corresponding $\Delta J(\mathcal{E})$ (right y axis) at $T=20$ K (a) and at 100 K (b). Full and empty symbols represent dc and pulsed measurements, respectively; dashed and solid lines represent the Ohmic regimes of $J(\mathcal{E})$ and power-law fits to $\Delta J(\mathcal{E})$, respectively. The insets show graphs for $y=0.25$ at 20 K and for $y=0$ at 100 K on a linear scale. (c) Fitting parameters α and $\mathcal{E}_o$ for various samples as functions of temperature. Pairs of full and empty symbols denote different samples of the same composition from the same batch, except for the two undoped samples ($y=0$) that belong to different batches. The dashed line represents the sample average of α as a function of T.

tions are shown in Fig. 3(c). With increasing temperature α rises from 2.2 ± 0.2 at 20 K to 2.53 ± 0.23 at 120 K; in this narrow range of values, α shows no correlation with composition. $\mathcal{E}_o$ rises superlinearly with temperature; at 20 K it is highest for an undoped sample (280 V/cm) and lowest for a sample doped with $y=0.25$ (46 V/cm), but depends weakly on y in the range $0.1\leqslant y\leqslant 0.25$. The values of α obtained in this work are practically identical with those found for the quasicubic $La_{0.7}Sr_{0.3}Mn_{1-y}Fe_yO_3$ (Ref. 5), but here the $\mathcal{E}_o$ are about one order of magnitude higher than those of the earlier system.

According to the GM model,[7] for $eV\gg k_BT$ the I-V dependence of a thin amorphous film is given by

$$I=(G_o+G_1)V+\sum_{n=2}^{\infty} a_n V^{n+1-2/(n+1)}. \tag{3}$$

Again the first two terms in Eq. (3) represent elastic tunneling, that is, direct and resonant tunneling via one impurity. The nonlinear terms represent inelastic, multistep tunneling via $n\geqslant 2$ impurities; the power index for $n=2$ is 7/3 and for $n=3$ it is 7/2. All values of α found in this work are very close to 7/3 at low T and do not deviate much from this value at higher temperatures. This indicates that (as in the case of $La_{0.7}Sr_{0.3}Mn_{1-y}Fe_yO_3$) the nonlinear conductivity of $La_{1.2}Sr_{1.8}Mn_{2-y}Cr_yO_7$ is dominated by inelastic tunneling across WLs (weak links) via pairs of impurity states. Our measurements were carried out at $T>T_2(1)$ [$T_2(1)=(A_1/B_1)^{3/4}$—see discussion above], thus WL1 are short circuited by inelastic tunneling activated thermally and by weak electric fields. It seems that the nonlinearity of the I-V characteristic is due to other weak links (represented here by WL2).

A lower limit of the distance l between successive WL2 may be estimated from the inequality $el\mathcal{E}_o\gg k_BT$. At 20 K, where $\alpha\approx 7/3$, we obtain $l\gg 6\times10^{-6}$ cm for the Cr-free sample and $l\gg 4\times10^{-5}$ cm for $y=0.25$.

B. Single crystals of $La_{1.4}Sr_{1.6}Mn_{1.85}Cr_{0.15}O_{7-\delta}$

1. Temperature dependence of resistivity and thermopower

Figures 4(a) and 4(b) show $\rho(T)$ and $S(T)$ for two single crystals of $La_{1.4}Sr_{1.6}Mn_{1.85}Cr_{0.15}O_{7-\delta}$ that grew in the same region of the original ingot. The single crystals, labeled SC1 and SC2, are platelets of dimensions $0.23\times0.19\times0.036$ and $0.37\times0.12\times0.08$ cm^3, respectively. $\rho(T)$ of SC1 resembles that of the polycrystals with $y\sim0.2$ [see Figs. 1(b) and 2(a)], but is lower by about two orders of magnitude. The resistivity of SC2 is even lower and it exhibits clearly a dip associated with the T_c. Both traces show a steep upturn at temperatures below 50 K. For SC1, between 50 and 100 K, there is a slight hysteresis but the main features were preserved during several cooling-heating cycles; the magnitude of the hysteresis decreased with repeated cycling indicating an aging process. Temperature-dependent memory effects in a single crystal of $(La_{0.4}Pr_{0.6})_{1.2}Sr_{1.8}Mn_2O_7$ were recently reported.[19] The low-temperature and low magnetic-field resistivities of that crystal are in the range of ρ of our SC1 and SC2 crystals.

The $S(T)$ traces of the two single crystals differ from those for the Cr-doped polycrystals in only minor details: for the single crystals, the temperatures of the zero crossing and of the maximum are slightly higher. The traces of $S(T)$ for

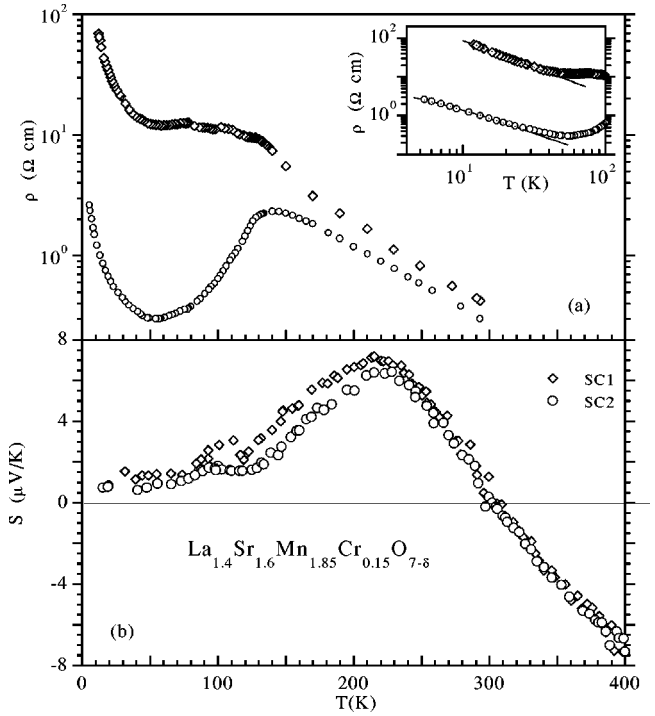

FIG. 4. (a) Temperature dependence of resistivity of two single crystals of $La_{1.4}Sr_{1.6}Mn_{1.85}Cr_{0.15}O_{7-\delta}$, crystal SC1 (upper trace $\diamondsuit$) and crystal SC2 (lower trace $\bigcirc$). The low-temperature portions of $\rho(T)$ are replotted in the inset on a log-log scale. (b) Temperature dependence of the absolute thermopower of the two crystals.

the two single crystals are almost identical in spite of the difference of more than one order of magnitude between their low-temperature resistivities. It seems that as before, $S(T)$ probes only the conducting component of the material, irrespective of the metal/nonmetal ratio or the density of weak links.

Here again the log-log plot of $\rho(T)$ shown in the inset of Fig. 4(a) brings into focus the low-temperature regime ($T<50$ K). The solid line in the upper trace (for SC1) represents $\rho \propto T^{-1.38}$; the negative power index, slightly higher than 4/3 may be associated with inelastic tunneling with mainly $n=2$ and some contribution from $n=3$. The lower solid line (for SC2) represents $\rho=(0.2+0.025T^{4/3})^{-1}$; for this sample $T_2=4.7$ K, which is comparable to that for the Cr-doped polycrystals with $y=0.2$. The similarities between $\rho(T)$ of the polycrystals and the single crystals are remarkable and indicate a similar mechanism in both types of samples. The shiny single crystals (which are flat under the electron microscope) do not contain grain boundaries. The weak links that govern their low-temperature resistivity are probably of intragrain origin. The presence of domain boundaries would account for the hysteresis.

2. J-$\mathcal{E}$ characteristics

Measurements of *I-V* characteristics over wide ranges of currents could be carried out only on sample SC1 at low temperatures (the resistivity of SC2 was too low for these measurements). The *J-*$\mathcal{E}$ characteristics are very nonlinear already at relatively low fields; the values of $\mathcal{E}_o$ range between ~ 0.1 V/cm at $T=10$ K to ~ 0.4 V/cm at 40 K, that is, more than two orders of magnitude lower than the lowest values of $\mathcal{E}_o$ obtained for our polycrystals [see Fig. 3(c)]. ΔJ vs $\mathcal{E}$ obtained for SC1 during its first cooling cycle, and after several cooling-heating cycles are plotted in Figs. 5(a) and 5(b), respectively. The results for the virgin sample [Fig. 5(a)] are simpler; the trace for 11.5 K exhibits a weak inflection at low fields and straightens up for the upper three decades of ΔJ while that for 30 K is a straight line over more than 5 decades. At high fields the straight lines are parallel with slopes that are close to the theoretical value for $n=2$ (i.e., $\alpha \sim 7/3$). Above $\mathcal{E} \sim 5$ V/cm the *I-V* characteristics for the virgin sample became erratic, although on the scale of milliseconds the pulses remained flat. After repeated thermal cycling the erratic response disappeared; this seems to be related to the decay of the hysteresis in $\rho(T)$. This erratic behavior reflects the fragility of the WLs network in virgin single crystals; each high-current pulse can make and break[20] part of the conduction paths. Reproducibility is eventually achieved upon aging.

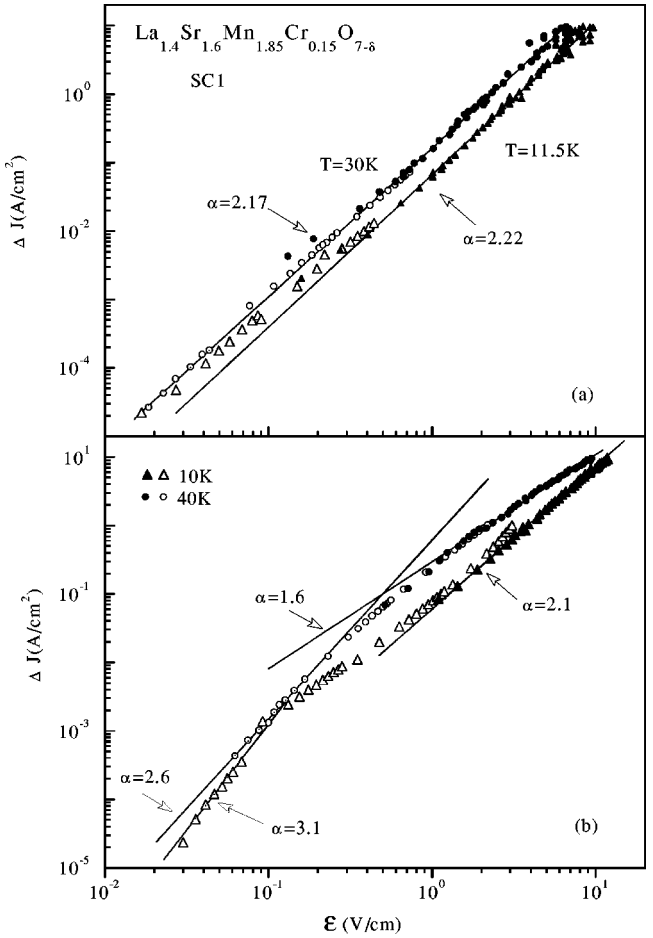

FIG. 5. $\Delta J(\mathcal{E})$ of single crystal SC1 at various temperatures, during first cooling (a), and after several cooling-heating cycles (b). Empty and full symbols represent dc and pulsed measurements, respectively.

The main feature of the graphs in Fig. 5(b) is an inflection between the two regimes; at low fields α decreases from 3.1 at 10 K to 2.6 at 40 K, at high fields it decreases from 2.1 for

10 K to 1.6 for 40 K. This behavior may be modeled in terms of the equivalent circuit in Fig. 2(b) that represents two types of WLs connected in series. At low fields the WLs with the highest resistances are probed. As $\mathcal{E}$ increases these are short-circuited by their field-activated inelastic tunneling, and other type(s) of WLs now dominate the *I-V* characteristic. The low value of α at the upper limit of the trace for 40 K indicates that at this temperature the transition from one type to other type(s) of WLs is far from being completed, even at the highest fields. We assume that the network of WLs in the single crystal consists of planar defects, such as domain boundaries. The presence of a domain structure was visualized[21] in the magneto-optical image of a single crystal of composition close to ours ($La_{1.36}Sr_{1.64}Mn_2O_7$). In polycrystalline manganites, the linear and nonlinear conductivities are probably governed by both intergrain and intragrain WLs, while in single crystals only by the latter. Irrespective of their origin, the behavior of the WLs is well explained by the GM model.

IV. SUMMARY

We reported here a systematic study of linear and nonlinear transport properties of ferromagnetic, polycrystalline $La_{1.2}Sr_{1.8}Mn_{2-y}Cr_yO_7$ ($y=0$, 0.1, 0.15, 0.2, and 0.25) in which low-T magnetization and resistivity are controlled by the Cr content. Linear transport measurements were carried out also on two weakly insulating single crystals of $La_{1.4}Sr_{1.6}Mn_2O_{7-\delta}$; pulsed *I-V* characteristics were measured only on the more resistive one. The results obtained from the measurements on the polycrystals as well as on the single crystals are consistent with the model of electronic transport along percolating paths embedded in an insulating matrix, with the percolating paths disrupted by (intergrain and intragrain) weak links. Analysis of the temperature dependence of resistivity and *I-V* characteristics indicates that the linear and nonlinear conductivities in both types of weakly insulating media are governed by inelastic tunneling through weak links, in accordance with the model of Glazman and Matveev[7] for inelastic, multistep tunneling across an amorphous thin film. The values of the parameter α in $\Delta J(=J-\sigma\mathcal{E})\propto\mathcal{E}^{\alpha}$, obtained here for bilayered manganites, are practically identical with those found for the quasicubic $La_{0.7}Sr_{0.3}Mn_{1-y}Fe_yO_3$ (Ref. 5), in further support of our earlier conclusion that the model for a single weak link may be extended to a network of weak links, irrespective of the dimensionality of the system. In the polycrystalline layered manganites the characteristic field for nonlinear conductivity $\mathcal{E}_o$ is roughly one order of magnitude higher than in the quasicubic manganites.[5] On the other hand, in the single crystal $J(\mathcal{E})$ becomes nonlinear already at comparatively low electric fields. This is probably due to much lower density of weak links in this crystal. The measurements of $\rho(T)$ and *I-V* characteristics in polycrystals are highly reproducible, while in the single crystal $\rho(T)$ exhibits hysteresis at low T and its *I-V* characteristic is erratic at fields above 5 V/cm. However, reproducibility is achieved upon aging.

ACKNOWLEDGMENTS

This research was supported by the Posnansky Research Fund for HTSC, the Center of Absorption in Science, the Ministry of Immigrant Absorption, and by the Fund for the Promotion of Research at Technion.

[1] M. Fäth, S. Freisem, A.A. Menovsky, Y. Tomioka, J. Aarts, and J.A. Mydosh, Science **285**, 1540 (1999), and references therein.

[2] M. Mayr, A. Moreo, J.A. Vergés, J. Arispe, A. Feiguin, and E. Dagotto, Phys. Rev. Lett. **86**, 135 (2001), and references therein.

[3] See, e.g., A. Carrington and J.R. Cooper Physica C **219**, 119 (1994).

[4] B. Fisher, J. Genossar, L. Patlagan, G.M. Reisner, and A. Knizhnik, Phys. Rev. B **59**, 8745 (1999), and references therein.

[5] K.B. Chashka, B. Fisher, J. Genossar, L. Patlagan, and G.M. Reisner, Phys. Rev. B **63**, 064403 (2001).

[6] For a review, see J.M.D. Coey M. Viret, and S. von Molnar, Adv. Phys. **48**, 167 (1999).

[7] L.I. Glazman and K.A. Matveev Zh. Éksp. Teor. Fiz. **94**, 332 (1988) [Sov. Phys. JETP **67**, 1276 (1988)].

[8] J. Klein, C. Höfener, S. Uhlenbruck, L. Alff, B. Büchner, and R. Gross, Europhys. Lett. **47**, 371 (1999); C. Höfener, J.B. Philipp, J. Klein, L. Alff, A. Marx, B. Büchner, and R. Gross, *ibid.* **50**, 681 (2000); R. Gross, L. Alff, B. Büchner, B.H. Freitag, C. Höfener, J. Klein, Yafeng Lu, W. Mader, J.B. Philipp, M.S.R. Rao, P. Reutler, S. Ritter, S. Thienhaus, S. Uhlenbruck, and B. Wiedenhorst, J. Magn. Magn. Mater. **211**, 150 (2000).

[9] Y. Moritomo, A. Asamitsu, H. Kuwahara, and Y. Tokura, Nature (London) **380**, 141 (1996).

[10] See e.g., M. Medarde, J.F. Mitchell, J.E. Millburn, S. Short, and J.D. Jorgansen, Phys. Rev. Lett. **83**, 1223 (1999); B. Garcia-Landa, C. Marquina, M.R. Ibarra, G. Balakrishnan, M.R. Lees, and D.McK. Paul, *ibid.* **84**, 995 (2000); K.V. Kamenev, M.R. Lees, G. Balakrishnan, D.McK. Paul, W.G. Marshall, V.G. Tissen, and M.V. Nefedova, *ibid.* **84**, 2710 (2000), and references therein.

[11] R. Gundakaram, J.G. Lin, F.Y. Lee, M.F. Tai, C.H. Shen, R.S. Liu, and C.Y. Huang, J. Phys.: Condens. Matter **11**, 5187 (1999).

[12] J.F. Mitchell, D.N. Argyriou, J.D. Jorgansen, D.G. Hinks, C.D. Potter, and S.D. Bader, Phys. Rev. B **55**, 63 (1997).

[13] Often, the possibility of Joule heating is rejected in the interpretation of high $\mathcal{E}$ effects measured in (weakly or strongly) insulating samples, when the measurements are carried out using current pulses of long duration or dc currents. This is supposedly justified by the negligible increase in the *average* temperature of the sample as calculated from the *average* power density.

[14] T. Ishikawa, K. Tobe, T. Kimura, T. Katsufuji, and Y. Tokura, Phys. Rev. B **62**, 12 354 (2000).

[15] N.F. Mott, Philos. Mag. **19**, 835 (1969).

[16] J.-S. Zhou, J.B. Goodenough, and J.F. Mitchell Phys. Rev. B **58**, R579 (1998).

[17] It is easy to show that the relation between the power index p and T_o is $p \approx (1/4)(T_o/T)^{1/4}$, where T is an average temperature in the range of the measurements. Here p increases almost linearly with y from $p=4.6$ for $y=0$ to $p=5.8$ for $y=0.25$; (the corresponding values of ${T_o}^{1/4}$ range between 71 and 88 $K^{1/4}$).

[18] See Eqs. (3.4)–(3.6) in Ref. 7.

[19] I. Gordon, P. Wagner, V.V. Moshchalkov, Y. Bruynseraede, M. Apostu, R. Suryanarayanan, and A. Revcolevschi, Phys. Rev. B **64**, 092408 (2001).

[20] This expression was taken from F.M. Hess, R.D. Merithew, M.B. Weissman, Y. Tokura, and Y. Tomioka, Phys. Rev. B **63**, 180408 (2001).

[21] U. Welp, A. Berger, V.K. Vlasko-Vlasov, Qing'An Li, K.E. Gray, and J.F. Mitchell, Phys. Rev. B **62**, 8615 (2000).